

Energy dependence of slope parameter in elastic nucleon-nucleon scattering

V.A. Okorokov ^a

National Research Nuclear University “MEPhI” (Moscow Engineering Physics Institute),
Kashirskoe Shosse 31, 115409 Moscow, Russia

September 30, 2018

Abstract. The study of slope parameter is presented for elastic proton-proton and antiproton-proton scattering with taking into account the recent experimental data at high energies. The expanded logarithmic approximations allow the description of the experimental slopes in all available energy range reasonably. Accounting for the LHC results leads to the dramatic change of behavior of the quadratic in logarithm approximation at high energies and to the closer trends for all fitting functions under study in comparison with the analysis at collision energies up to the 200 GeV. The estimations of the asymptotic shrinkage parameter $\alpha'_{\mathcal{P}}$ are discussed. Predictions for diffraction slope parameter are obtained for some proton-proton and antiproton-proton facilities.

PACS. 13.75.Cs Nucleon-nucleon interactions – 13.85.Dz Elastic scattering

1 Introduction

The one of the important quantity for nucleon elastic scattering is the slope parameter B which is defined in accordance with the following equation:

$$B(s, t) = \partial_t \ln \partial_t \sigma(s, t), \quad (1)$$

where $\partial_t \equiv \partial/\partial t$. The B is determined experimentally by fitting the differential cross section $d\sigma/dt$ at some collision energy \sqrt{s} . The study of B parameter is important, in particular, for reconstruction procedure of full set of helicity amplitudes for elastic nucleon-nucleon scattering [1]. In the last 20–30 years, high-energy $\bar{p}p$ colliders have extended the maximum $\bar{p}p$ collision energy from $\sqrt{s} \sim 20$ GeV to $\sqrt{s} \sim 2$ TeV, the LHC facility allows one to obtain pp data up to $\sqrt{s} = 8$ TeV so far. As consequence, the available collection of pp and $\bar{p}p$ slope data from literature has extended. The $B(s)$ for elastic pp and $\bar{p}p$ reactions is under consideration below. Within the classical Regge model the Pomeron trajectory, $\alpha_{\mathcal{P}}(t)$, is linear function of momentum transfer, i.e. $\alpha_{\mathcal{P}}(t) = \alpha_{\mathcal{P}}(0) + \alpha'_{\mathcal{P}}t$. Therefore using the definition (1) the following relation can be obtained for $B(s)$ at some fixed t :

$$B(s) \propto 2\alpha'_{\mathcal{P}} \ln \varepsilon,$$

where $\varepsilon \equiv s/s_0$, $s_0 = 1$ GeV². In general case for Pomeron-inspired models the asymptotic shrinkage parameter $\alpha'_{\mathcal{P}}$ can be written as follows: $2\alpha'_{\mathcal{P}}(s) = \partial_{\ln \varepsilon} B(s, t)$.

2 Experimental slope energy dependence

As in the previous analyses [2,3,4] dependence $B(s)$ is parameterized by the following analytic functions:

$$B(s, t) = B_0 + 2a_1 \ln \varepsilon, \quad (2a)$$

$$B(s, t) = B_0 + 2a_1 \ln \varepsilon + a_2 \ln^{a_3} \varepsilon, \quad (2b)$$

$$B(s, t) = B_0 + 2a_1 \ln \varepsilon + a_2 \varepsilon^{a_3}, \quad (2c)$$

$$B(s, t) = B_0 + 2a_1 \ln \varepsilon + a_2 \ln^2 \varepsilon, \quad (2d)$$

where free parameters B_0 , a_i , $i = 1 - 3$ depend on range of $|t|$ which is used for approximation. There are the relations $\alpha'_{\mathcal{P}} = a_1$ and $\alpha'_{\mathcal{P}} = a_1 + a_2 \ln \varepsilon$ for parameterizations (2a) and (2d) inspired by the Pomeron exchange models. Appendix shows database of available experimental results for slope parameter in elastic $pp/\bar{p}p$ scattering. The some numerical values of the $B(s, t)$ from this database are used in the present study. Experimental values of slope parameter collected at initial energies $\sqrt{s} \leq 1.8$ TeV were used in [4]. Additional experimental results from Tevatron and the LHC are from [91] and [39,40,41,53], respectively. The full data sample consists of 490 experimental points. The number of experimental points is equal 145/138 (137/70) for $pp/\bar{p}p$ scattering at low (intermediate) $|t|$ respectively. It should be noted that for intermediate $|t|$ range the experimental results for $B(s)$ obtained with help of linear parametrization for logarithm of differential cross-section, $\ln(d\sigma/dt) \propto (-B|t|)$, are discussed below because the new experimental data at intermediate $|t|$ [53,91] with respect to the [4] are obtained for such parametrization of $\ln(d\sigma/dt)$ namely. From the exponential parametrization with index quadratic in t for differential cross-section,

^a e-mail: VAOkorokov@mephi.ru; Okorokov@bnl.gov

$\ln(d\sigma/dt) \propto (-B|t| \pm Ct^2)$, one may calculate the local slope as following

$$b(s, t)|_{|t|=0.2\text{GeV}^2} = B \pm C \ln |t|, \quad B, C > 0. \quad (3)$$

In accordance with [4] the mean value of $|t|$ ($|\bar{t}|$) is calculated with taking into account the approximation of experimental $d\sigma/dt$ distribution; errors of experimental points include available clear indicated systematic errors added in quadrature to statistical ones. The fitting algorithm is described in detail in [4]. As previously the points with $n_\chi \geq 2$ are excluded from fit in our algorithm, where [4]

$$n_\chi = \left(\frac{B_m^i - B(s_i; \alpha)}{\sigma_i \sqrt{\chi^2/\text{n.d.f.}}} \right)^2. \quad (4)$$

Here B_m^i is the measured value of nuclear slope at s_i with experimental error σ_i , $B(s_i; \alpha)$ is the expected value from the fitting function with best $\chi^2/\text{n.d.f.}$ among (2a) – (2d) for approximation of all range of available energies, the parameters α_j are from N -dimensional vector $\alpha = \{\alpha_1, \dots, \alpha_N\}$. We consider the estimates of fit parameters as the final results if there are no excluded points for present data sample. The fraction of excluded points is about 2% for pp as well as for $\bar{p}p$ elastic scattering for low $|t|$ domain. The maximum relative amount of rejected points is about 3%/12% for linear $\ln d\sigma/dt$ parametrization at intermediate $|t|$ values for $pp/\bar{p}p$ scattering respectively.

2.1 Low $|t|$ domain

The experimental dependence $B(s)$ and corresponding fits by (2a) – (2d) are shown in Fig.1 for elastic pp scattering, Table 1 contains values of fit parameters. As seen the fitting functions (2a), (2d) describe the pp experimental data statistically acceptable only for $\sqrt{s} \geq 5$ GeV. The RHIC point at $\sqrt{s} = 200$ GeV does not contradict the common trend within a large error bars and can't discriminate the approximations under study. In general the LHC results [39,41,40] added in fitting sample result in better agreement of fits (2a) – (2d) in comparison with previous study [4]. All fits are very close to each other in energy domain $10 \text{ GeV} \lesssim \sqrt{s} \lesssim 1 \text{ TeV}$, the quadratic in logarithm function (2d) shows some faster increasing of slope and noticeable difference from another fit functions in multi-TeV region only. It seems the ultra-high energy domain is suitable for separation of various parameterizations. Fitting functions (2b), (2c) allow us to describe experimental data at all energies with reasonable fit quality for pp (Table 1). The functions (2a) – (2c) agrees very well for $\sqrt{s} \geq 5$ GeV, furthermore there is no visible difference between modifications (2b) and (2c) in all experimentally available energy domain. The function (2c) demonstrate some better quality for fit of full data sample (Table 1) than function (2b) in contrast with previous analysis [4]. The mean value of (4) for excluded points (\bar{n}_χ) is equal 4.7 for pp data sample for parametrization (2c). The accounting for LHC data

leads to some decreasing of values of B_0 and increasing of a_1 parameters for all fitting functions (2a) – (2d) under study in comparison with values of corresponding parameters in previous investigation [4]. This behavior of a_1 with collision energy agrees well with predicted growth of α'_p with increasing of \sqrt{s} [75,94]. As seen from Table 1 the third term in both the (2b) and the (2c) gives the main contribution at $\sqrt{s} < 5$ GeV in the case of elastic proton-proton scattering, i.e. describe the sharp changing of slope in the low energy domain. Therefore $B^{pp} \propto \ln \varepsilon$ at high \sqrt{s} in accordance with (2b) and (2c). Such asymptotic behavior is in qualitative agreement with energy dependence of the slope parameter for $\bar{p}p$ collisions [4]. The increasing of a_1 exhibits that B^{pp} growth some faster in multi-TeV region than one can expect from the trend based on data sample at $\sqrt{s} \leq 200$ GeV. This suggestion is confirmed by improvement of fit quality for one fitting function (2d) for present data sample in comparison with fit qualities for experimental points at $\sqrt{s} \leq 200$ GeV [4]. Values of a_2 obtained in present study and for fit at $\sqrt{s} \leq 200$ GeV are close within errors for functions (2b) and (2d) but accounting for the LHC data results in some increasing of the absolute value of a_3 in fit by (2b). The absolute values of a_2 and a_3 are the same within error bars for function (2c) for Table 1 and for fit in energy domain $\sqrt{s} \leq 200$ GeV [4].

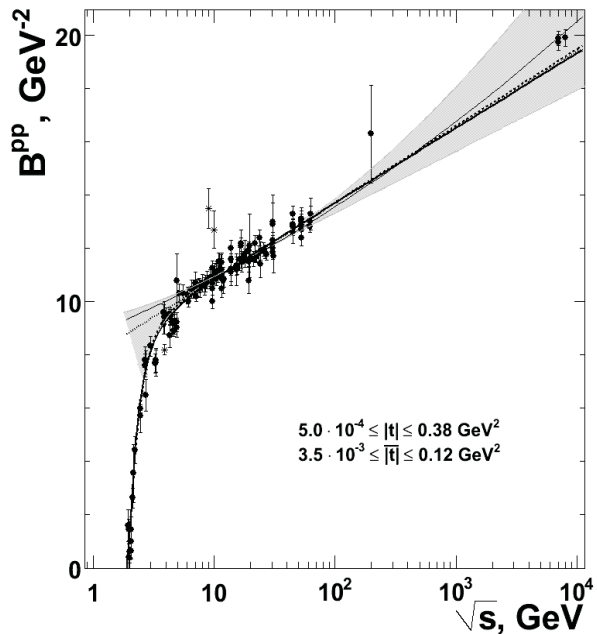


Fig. 1. Energy dependence of the slope parameter for elastic pp scattering for low $|t|$ domain. Experimental points from fitted samples are indicated as \bullet , unfitted points are indicated as $*$. The dot curve is the fit of experimental slope by the function (2a), thick solid – by the (2b), dashed – by the (2c), thin solid – by the (2d). The shaded band corresponds to the spread of fitting functions for previous analysis [4].

Table 1. Values of parameters for fitting of slope energy dependence in pp elastic scattering for low $|t|$ domain

Function	Parameter				
	B_0, GeV^{-2}	a_1, GeV^{-2}	a_2, GeV^{-2}	a_3	$\chi^2/\text{n.d.f.}$
(2a)	8.00 ± 0.06	0.309 ± 0.010	–	–	234/98
(2b)	8.09 ± 0.06	0.305 ± 0.005	-31.8 ± 1.6	-4.06 ± 0.13	420/138
(2c)	7.95 ± 0.06	0.313 ± 0.005	-240 ± 32	-2.23 ± 0.09	402/138
(2d)	8.81 ± 0.12	0.198 ± 0.015	0.013 ± 0.002	–	174/97

Table 2. Predictions for slope in nucleon-nucleon elastic scattering at intermediate energies for low $|t|$ domain

Fitting function	Facility energies \sqrt{s}, GeV					
	FAIR			NICA		
	3	5	6.5	14.7	20	25
(2a)	–	11.4 ± 0.2	11.6 ± 0.2	12.3 ± 0.2	11.70 ± 0.13	11.98 ± 0.14
(2b)	12.57 ± 0.07	12.80 ± 0.07	12.93 ± 0.07	13.32 ± 0.09	11.72 ± 0.08	12.00 ± 0.09
(2c)	12.59 ± 0.05	12.83 ± 0.06	12.95 ± 0.06	13.34 ± 0.07	11.70 ± 0.08	11.98 ± 0.09
(2d)	–	11.9 ± 1.2	12.0 ± 1.3	12.4 ± 1.6	11.6 ± 0.2	11.9 ± 0.2

Table 3. Predictions for slope in pp elastic scattering at high energies for low $|t|$ domain

Fitting function	Facility energies \sqrt{s}, TeV						
	RHIC		LHC		FCC/VLHC		
	0.5	14	28	42*	100	200	500
(2a)	15.7 ± 0.3	19.8 ± 0.4	20.7 ± 0.4	21.2 ± 0.4	22.2 ± 0.5	23.1 ± 0.5	24.2 ± 0.5
(2b)	15.67 ± 0.14	19.7 ± 0.2	20.6 ± 0.2	21.1 ± 0.2	22.1 ± 0.2	23.0 ± 0.3	24.1 ± 0.3
(2c)	15.73 ± 0.14	19.9 ± 0.2	20.8 ± 0.2	21.3 ± 0.2	22.4 ± 0.2	23.2 ± 0.3	24.4 ± 0.3
(2d)	15.7 ± 0.5	21.1 ± 0.9	22.4 ± 1.0	23.1 ± 1.1	24.8 ± 1.3	26.2 ± 1.4	28.2 ± 1.6

*The ultimate energy upgrade of LHC project [96].

The comparison with earlier studies [95,21] confirms the conclusion above that accounting for high energy data points leads to increasing of value of a_1^{pp} parameter and growth of slope parameter seems to be faster in TeV-region than that at lower energies. Accordingly the a_1^{pp} value for function (2d) is closer significantly to the $\alpha'_p \approx 0.25 \text{ GeV}^{-2}$ than that for previous analysis in energy range $\sqrt{s} \leq 200 \text{ GeV}$ [4]. On the other hand the values of the a_1^{pp} parameter obtained for fitting function (2a) is some larger than the prediction for α'_p from Pomeron inspired model for TeV-energy domain [94]. Furthermore the proton-proton results from fit by function (2d) allow the estimation $2\alpha'_p(s)|_{\sqrt{s}=8\text{TeV}} = 0.86 \pm 0.08$ which is almost twice larger than the corresponding prediction from [94].

Predictions for B are obtained for some facilities based on the fit results shown above for pp and on the results from [4] for $\bar{p}p$. Estimations at low $|t|$ for different intermediate energies of the projects FAIR and NICA are shown in the Table 2 and for high energy domain are presented in the Table 3. As expected the functions (2b) and (2c) predicts for FAIR the B values coincide with each other within errors. The approximation functions (2a) and (2d) can predict for $\sqrt{s} \geq 5 \text{ GeV}$ only. The Pomeron inspired function (2a) predicts slope parameter values smaller significantly than that for modified fitting functions (2b) and (2c) at FAIR energies. For $\bar{p}p$ the predictions with help

of quadratic in $\ln \varepsilon$ function (2d) are equal with estimations based on any another fitting function under study within large error bars at $\sqrt{s} \leq 14.7 \text{ GeV}$. In the case of elastic pp scattering the functions (2a) – (2c) predict just the equal values of B within error bars at any collision energy \sqrt{s} discussed here. The difference between estimations from (2a) – (2c) and from (2d) onsets at the final energy of the LHC project $\sqrt{s} = 14 \text{ TeV}$ only. Our prediction with (2d) function for RHIC energy is equal with early prediction for close energy based only on slope data in the region $5 < \sqrt{s} < 62 \text{ GeV}$ [97] within errors. But (2d) underestimates the B values in ultra-high energy domain $\sqrt{s} > 40 \text{ TeV}$ in comparison with results based on the approach without odderons [97]. It should be emphasized that in contrast with previous analysis [4] the present fits by functions (2a) – (2d) of data sample included of the LHC results predict the similar increasing of B with energy as most of phenomenological models [98]. The B value predicted for the LHC at $\sqrt{s} = 14 \text{ TeV}$ by (2a) only is close with errors to the predictions from [99,100], in particular, with estimation from model with hadronic amplitude corresponding to the exchange of two pomerons. Prediction of phenomenological model with hadronic amplitude corresponding to the exchange of three pomerons [100] at $\sqrt{s} = 14 \text{ TeV}$ coincides with estimation of B within error bars from fit function (2d) with fastest growth of B with \sqrt{s} in multi-TeV region. But

most of estimations of B at $\sqrt{s} = 14$ TeV from Table 3 agree well within errors with model prediction from [101]. However the model estimates at $\sqrt{s} = 14$ TeV described above were obtained for $B(t=0)$ and the t -dependence of slope shows the slight decreasing of B for the model with three-pomeron exchange [100] and faster decreasing of B for the model from [101] at growth of momentum transfer up to $|t| \approx 0.1$ GeV². Therefore one can expect that the model with hadronic amplitude corresponding to the exchange of three pomerons [100] will be in the better agreement with values of B from Table 3 predicted for finite (non-zero) low $|t|$ values. But the model from [102] overestimates the B value at $\sqrt{s} = 14$ TeV in comparison with corresponding predictions from fitting functions (2a) – (2d) despite of the sharp decreasing of B at growth of momentum transfer up to $|t| \approx 0.1$ GeV² in this model. As suggested sometimes the saturation regime, Black Disk Limit (BDL), maybe reach at the LHC. The one of the models in which such effects appear, namely, Dubna Dynamical Model (DDM) predicts the slope $B(t=0) \approx 23.5$ GeV⁻² at $\sqrt{s} = 14$ TeV [103] which is larger noticeably than the predictions from Table 3 at the same \sqrt{s} . Therefore the saturation regime will not be reached, at least, at the LHC energy $\sqrt{s} = 14$ TeV as suggested, for example, in the model from [104] or simple saturation can not be enough in order to describe the LHC data at quantitative level.

2.2 Intermediate $|t|$ domain

As indicated in [4] the situation is more complicated for intermediate $|t|$ domain. Figure 2 shows the experimental data and corresponding fits for energy dependence of slope parameter at intermediate $|t|$ for exponential approximation with index linear in $|t|$ of differential cross-sections in elastic pp and $\bar{p}p$ scattering. The parameter values for fitting are indicated in Table 4 for various interaction types.

Usually the fit qualities are poorer for intermediate $|t|$ values than that for low $|t|$ range in pp elastic collisions for linear parametrization of $\ln(d\sigma/dt)$. The fitting functions (2a) and (2d) agree with experimental points qualitatively for $\sqrt{s} \geq 5$ GeV only. Furthermore in the first case there is significant discrepancy between experimental point and fit curve at the LHC energy also (Fig.2a). The “expanded” functions (2b), (2c) approximate experimental data at all energies reasonably with close fit qualities (Table 4), but these functions show a slow growth of slope parameter with energy increasing at $\sqrt{s} \geq 100$ GeV (Fig.2a). It should be stressed that the experimental point at the LHC energy leads to the dramatic change of behavior of the fitting function (2d) in comparison with previous analysis [4]. At present the fitting function (2d) predicts increasing of the nuclear slope in high energy domain as well as all other fitting functions under study. Such behavior is opposite to the result of fit by function (2d) of experimental data sample at $\sqrt{s} \leq 200$ GeV [4]. As shown in previous analysis [4] the the $\bar{p}p$ experimental data admit the approximation by (2a), (2d) for all energy range but not only for $\sqrt{s} \geq 5$ GeV (Fig.2b). Thus

the parameter values are shown in Table 4 for approximation by (2a), (2d) of all available experimental data. The fit curves show (very) close behaviors for both the present and previous analyses in the case of the Fig.2b. The $\bar{p}p$ data disagreement with Pomeron inspired fitting function (2a) very significantly (Fig.2b). Functions (2b) and (2c) show a close behavior at all energies for $\bar{p}p$ data from linear parametrization of $\ln d\sigma/dt$. These fitting functions have a better fit quality than (2d) but fits by functions (2b), (2c) are still statistically unacceptable. The $\bar{n}_\chi = 2.9$ for excluded pp data with (2c) function and $\bar{n}_\chi = 18.3$ for points excluded from $\bar{p}p$ fitted data sample for (2b) fitting function. As seen from Fig.2b behavior of the energy dependence of slope parameter for elastic $\bar{p}p$ scattering is close to the quadratic in logarithm function $B^{\bar{p}p} \propto \ln^2 \varepsilon$ at high \sqrt{s} as well as for elastic pp collisions. But in the last case it is difficultly to make the unambiguous conclusion because there is only the LHC point in the asymptotic region. The estimations of asymptotic shrinkage parameter are following for fitting functions (2a) and (2d) respectively: $2\alpha'_p = 0.422 \pm 0.016$ and $2\alpha'_p(s)|_{\sqrt{s}=7\text{TeV}} = 1.66 \pm 0.19$ for pp ; $2\alpha'_p = 0.272 \pm 0.008$ and $2\alpha'_p(s)|_{\sqrt{s}=1.96\text{TeV}} = 1.36 \pm 0.10$ for $\bar{p}p$. The values of α'_p are equal within errors at $\sqrt{s} = 7$ TeV and $\sqrt{s} = 8$ TeV for domain of $|t|$ under consideration in the case of the function (2d) for pp interaction. As seen from comparison with results from Table 1 for elastic pp collisions and from [4] for $\bar{p}p$ scattering the fitting function (2a) is characterized by smaller asymptotic shrinkage parameter for intermediate $|t|$ domain than that at small $|t|$ values while the situation for quadratic in logarithm function (2d) is opposite: there is significant growth of α'_p for transition from small $|t|$ to intermediate $|t|$ values.

We have obtained predictions for nuclear slope parameters B and b for some facilities and intermediate $|t|$. The B values are calculated on the base of fit results shown above. Estimations for b are obtained on the base of results from [4] with all functions under consideration with exception of the (2b). In the last case the following results are obtained within framework of the present analysis for $b(s)$: $B_0 = 9 \pm 2$ (50.8 \pm 0.9) GeV⁻², $a_1 = 0.19 \pm 0.12$ (0.92 \pm 0.06) GeV⁻², $a_2 = -10 \pm 2$ (-34.1 \pm 0.8) GeV⁻², $a_3 = -1.9 \pm 0.5$ (0.222 \pm 0.016), $\chi^2/\text{n.d.f.} = 41.4/33$ (8.7/15) for pp ($\bar{p}p$) data samples, respectively. Slope values are shown in the Table 5 for different energies of FAIR, NICA, and in the Table 6 for RHIC, LHC and FCC/VLHC. According to the fit range function (2a) can predicts the B value for $\bar{p}p$ scattering at all energies under study not in $\sqrt{s} \geq 5$ GeV domain only. As expected the functions (2b) – (2d) predicted very close values for slope parameter B for FAIR. These fitting functions, especially (2b) and (2c), predict the close values for nuclear slope B in NICA energy domain too. Functions (2a) – (2c) predict smaller values for B in high-energy pp collisions than (2d) approximation especially for FCC/VLHC energy domain. Perhaps, the future more precise RHIC results will be useful for discrimination of fitting functions under study for intermediate $|t|$ values. In the contrast with previous analysis [4], here the function (2d) with obtained parameters predicts

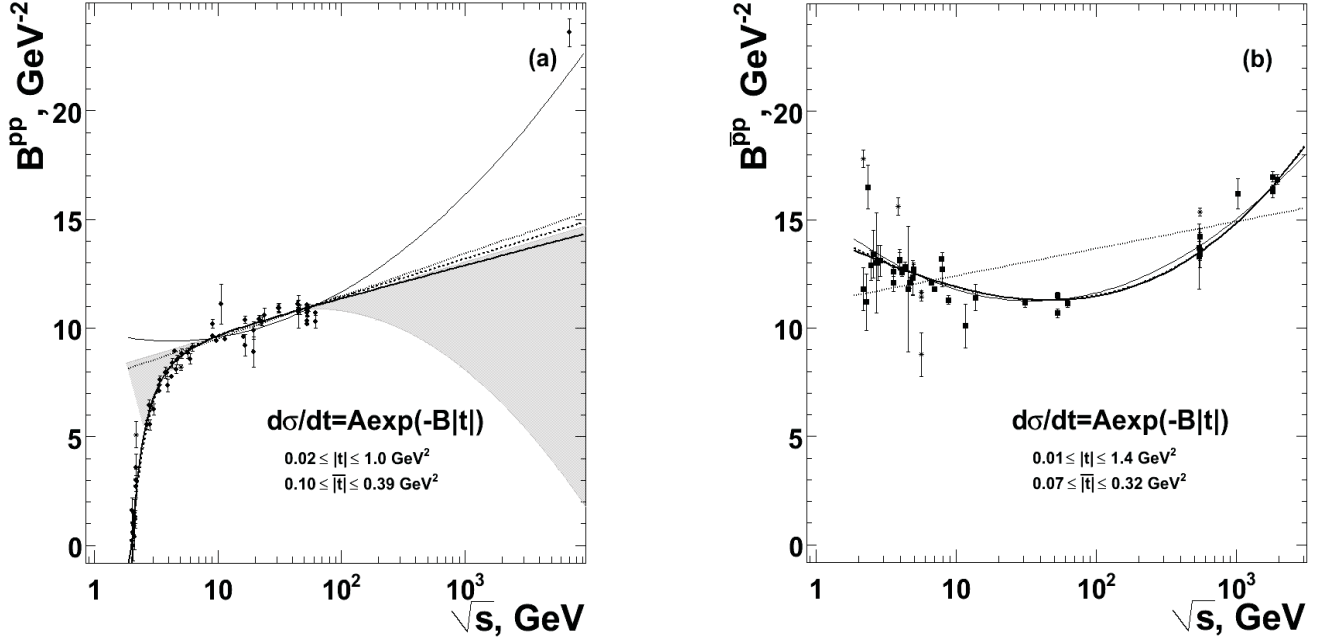


Fig. 2. Energy dependence of B in proton-proton (a) and antiproton-proton (b) elastic scattering for exponential parametrization with index linear in $|t|$ of differential cross section. Experimental points from fitted samples are indicated as close circles / squares for $pp/\bar{p}p$, unfitted points are indicated as *. The dot curve is the fit of experimental slope by the function (2a), thick solid – by the (2b), dashed – by the (2c), thin solid – by the (2d). The shaded band (a) corresponds to the spread of fitting functions for previous analysis [4].

Table 4. Values of parameters for fitting of energy dependence of slope at intermediate $|t|$

Function	Parameter				
	B_0, GeV^{-2}	a_1, GeV^{-2}	a_2, GeV^{-2}	a_3	$\chi^2/\text{n.d.f.}$
proton-proton scattering, experimental data for $d\sigma/dt = A \exp(-B t)$					
(2a)	7.59 ± 0.11	0.211 ± 0.008	–	–	322/35
(2b)	8.39 ± 0.17	0.163 ± 0.011	-25.2 ± 1.4	-3.01 ± 0.13	493/61
(2c)	7.94 ± 0.11	0.19 ± 0.09	-90 ± 8	-1.69 ± 0.06	458/61
(2d)	9.9 ± 0.2	-0.16 ± 0.03	0.056 ± 0.005	–	187/34
antiproton-proton scattering, experimental data for $d\sigma/dt = A \exp(-B t)$					
(2a)	11.16 ± 0.06	0.136 ± 0.004	–	–	1168/42
(2b)	14.34 ± 0.11	-0.304 ± 0.014	0.0042 ± 0.0004	2.92 ± 0.04	186/40
(2c)	7.7 ± 0.2	-0.735 ± 0.019	6.9 ± 0.2	0.1000 ± 0.0013	188/40
(2d)	15.48 ± 0.15	-0.60 ± 0.02	0.084 ± 0.003	–	197/41

Table 5. Predictions for slopes in nucleon-nucleon elastic scattering at intermediate energies for intermediate $|t|$ domain

Fitting function	Facility energies \sqrt{s} , GeV					
	FAIR				NICA	
	3	5	6.5	14.7	20	25
B -parameter						
(2a)	11.76 ± 0.06	12.04 ± 0.07	12.18 ± 0.07	12.62 ± 0.07	10.12 ± 0.15	10.31 ± 0.15
(2b)	12.88 ± 0.13	12.51 ± 0.14	12.26 ± 0.15	11.6 ± 0.2	10.2 ± 0.2	10.4 ± 0.2
(2c)	13.1 ± 0.3	12.5 ± 0.4	12.2 ± 0.4	11.6 ± 0.5	10.2 ± 1.1	10.4 ± 1.2
(2d)	13.27 ± 0.18	12.5 ± 0.2	12.2 ± 0.2	11.5 ± 0.3	10.0 ± 0.5	10.1 ± 0.5
b -parameter						
(2a)	10.0 ± 0.2	10.5 ± 0.2	10.7 ± 0.3	11.4 ± 0.3	10.5 ± 0.3	10.8 ± 0.4
(2b)	14.3 ± 1.4	12.6 ± 1.7	12.0 ± 1.8	11 ± 2	10 ± 2	11 ± 3
(2c)	14 ± 3	13 ± 3	12 ± 3	11 ± 3	10.5 ± 1.1	10.7 ± 1.2
(2d)	12.6 ± 1.1	12.0 ± 1.2	11.8 ± 1.3	11.3 ± 1.7	10 ± 2	11 ± 3

Table 6. Predictions for slopes in pp elastic scattering at high energies for intermediate $|t|$ domain

Fitting function	Facility energies \sqrt{s} , TeV						
	RHIC		LHC		FCC/VLHC		
	0.5	14	28	42*	100	200	500
B -parameter							
(2a)	12.8 ± 0.2	15.6 ± 0.3	16.2 ± 0.3	16.6 ± 0.4	17.3 ± 0.4	17.9 ± 0.4	18.7 ± 0.4
(2b)	12.4 ± 0.3	14.6 ± 0.4	15.1 ± 0.5	15.3 ± 0.5	15.9 ± 0.5	16.3 ± 0.6	16.9 ± 0.6
(2c)	13 ± 2	15 ± 3	16 ± 4	16 ± 4	17 ± 4	17 ± 4	18 ± 5
(2d)	14.5 ± 1.1	24 ± 2	27 ± 2	28 ± 3	32 ± 3	35 ± 3	40 ± 4
b -parameter							
(2a)	14.6 ± 0.6	18.8 ± 0.9	19.7 ± 1.0	20.2 ± 1.0	21.3 ± 1.1	22.2 ± 1.1	23.3 ± 1.2
(2b)	13 ± 4	16 ± 5	16 ± 5	17 ± 5	17 ± 6	18 ± 6	18 ± 6
(2c)	13.7 ± 1.9	17 ± 3	18 ± 3	18 ± 3	19 ± 3	20 ± 3	21 ± 4
(2d)	12 ± 5	9 ± 9	8 ± 10	7 ± 11	6 ± 12	4 ± 13	2 ± 14

*The ultimate energy upgrade of LHC project [96].

fast growth of B values at energies of future experiments. This behavior of estimations calculated for functions (2a) – (2d) contradicts with earlier predictions from some phenomenological models. It should be emphasized that various phenomenological models predict a very sharp decreasing of nuclear slope in the range $|t| \sim 0.3 - 0.5$ GeV² at LHC energy $\sqrt{s} = 14$ TeV [98]. Just the positive B value predicted for LHC at $\sqrt{s} = 14$ TeV by (2d) is most close to the some model expectations [100,101]. Taking into account predictions in Table 2 based on the fitting functions (2a) – (2d) for low $|t|$ one can suggest that the model with hadronic amplitude corresponding to the exchange of three pomerons [98,100] describes the nuclear slope some closer to the experimentally inspired values at LHC energy both at low and intermediate $|t|$ than other models. The situation with predictions for b at intermediate energies is similar to that for B : functions (2b) – (2d) predict close values for b within large errors for both the FAIR and the NICA. Furthermore all fitting functions predict the close values of b at $\sqrt{s} > 5$ GeV. The value of b parameter obtained from function (2a) differs significantly from estimations with other fitting functions for $\bar{p}p$ elastic scattering at low energies. Therefore the b parameter seems more perspective for distinguishing of Pomeron inspired function (2a) from “expanded” parameterizations (2b) – (2c) at $\sqrt{s} \sim 3$ GeV than B . One can see the functions (2b) and (2c) predict very close values of b in high-energy domain. Function (2d) shows a decreasing of b at high energies in the contrast with B parameter. In general estimations obtained with help of all fitting functions are agree within errors up to the $\sqrt{s} = 28$ TeV. But the large errors for function (2d) do not allow the unambiguous physics conclusion especially at the LHC energies and above.

2.3 ΔB and NN data analysis

In accordance with rules from [4] the difference of slopes (ΔB) for antiproton-proton and proton-proton elastic scattering is calculated for each function (2a) – (2d) under study with parameters from corresponded $\bar{p}p$ and pp fits:

$\Delta B_i(s) = B_i^{\bar{p}p}(s) - B_i^{pp}(s)$, $i = (2a) - (2d)$. The energy dependence of ΔB is shown at Fig.3a and Fig.3b for low and intermediate $|t|$ respectively. One can see that the difference of slopes decreasing with increasing of energy for low $|t|$ domain (Fig.3a) as well as in the previous analysis [4]. The fitting functions (2b), (2c) demonstrate much faster decreasing of ΔB with increasing of \sqrt{s} than that the functions (2a) and (2d). At present the proton-proton experimental data at highest available energy 8 TeV don't contradict with fast (square of logarithm of energy) increasing of slope at high energies in general case. Such behavior could be agreed with the asymptotic growth of total cross section. Furthermore in contrast with the previous analysis [4], here the quadratic in $\ln \varepsilon$ function (2d) leads to much smaller difference ΔB for $\bar{p}p$ and pp scattering in high energy domain for both low (Fig.3a) and intermediate (Fig.3b) values of $|t|$. The Pomeron inspired function (2a) only predicts the decreasing of ΔB with energy growth at intermediate $|t|$ (Fig.3b) for any values of \sqrt{s} . The parameterizations (2b) – (2d) predict the decreasing of difference of slopes at low and intermediate energies and fast increasing of ΔB at high energies for intermediate $|t|$ domain (Fig.3b). As expected the most slow changing of ΔB is predicted by Pomeron inspired function (2a) at asymptotic energies. All fitting functions with experimentally inspired parameters don't predict the constant zero values of ΔB at high energies. But it should be emphasized that only separate fits were made for experimental data for pp and $\bar{p}p$ elastic reactions above. These results indicate on the importance of investigations at ultra-high energies both pp and $\bar{p}p$ elastic scattering for study of many fundamental questions and predictions related to the general asymptotic properties of hadronic physics.

Also we have analyzed general data samples for pp and $\bar{p}p$ elastic scattering. Slope parameters (B and b) shows a different energy dependence at $\sqrt{s} < 5$ GeV in proton-proton and antiproton-proton elastic reactions in any $|t|$ domains under study. Thus slopes for nucleon-nucleon data are investigated only for $\sqrt{s} \geq 5$ GeV below. We have included in fitted samples only pp and $\bar{p}p$ points which have been included in corresponding final data samples at separate study pp and $\bar{p}p$ elastic reactions

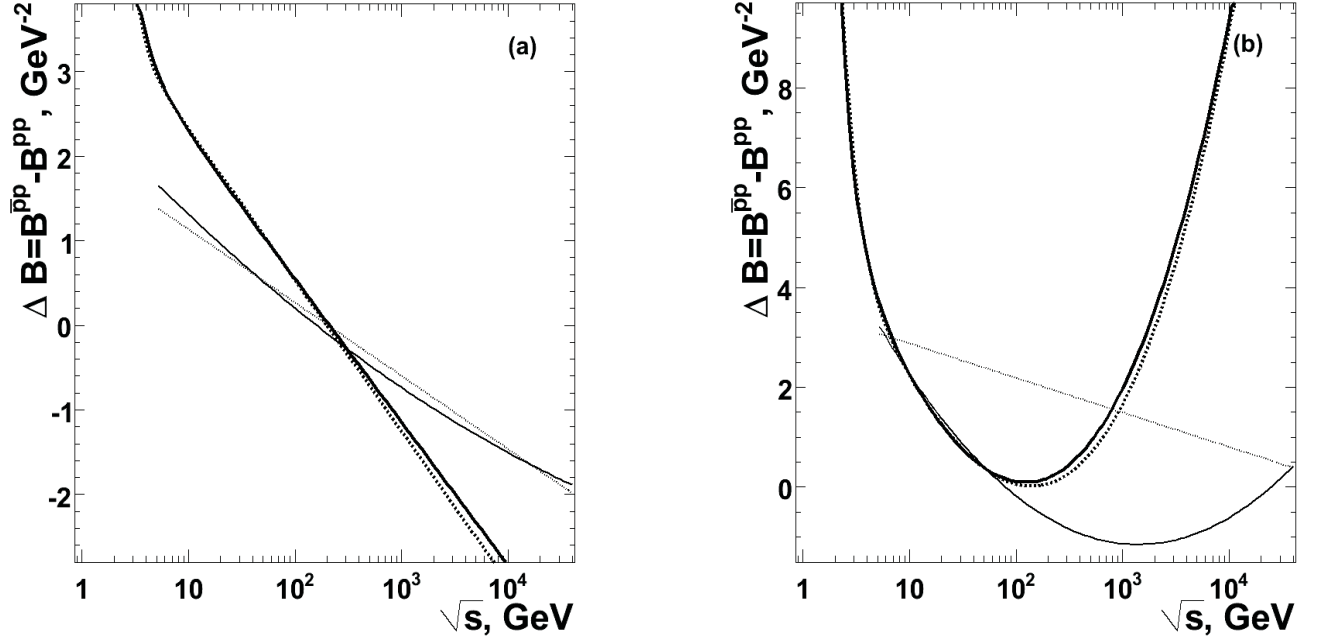


Fig. 3. The energy dependence of the difference of elastic slopes for antiproton-proton and proton-proton scattering in low $|t|$ domain (a) and in intermediate $|t|$ range for exponential fit with index linear in $|t|$ of differential cross-section (b). The correspondence of curves to the fit functions is the same as well as in Figure 1.

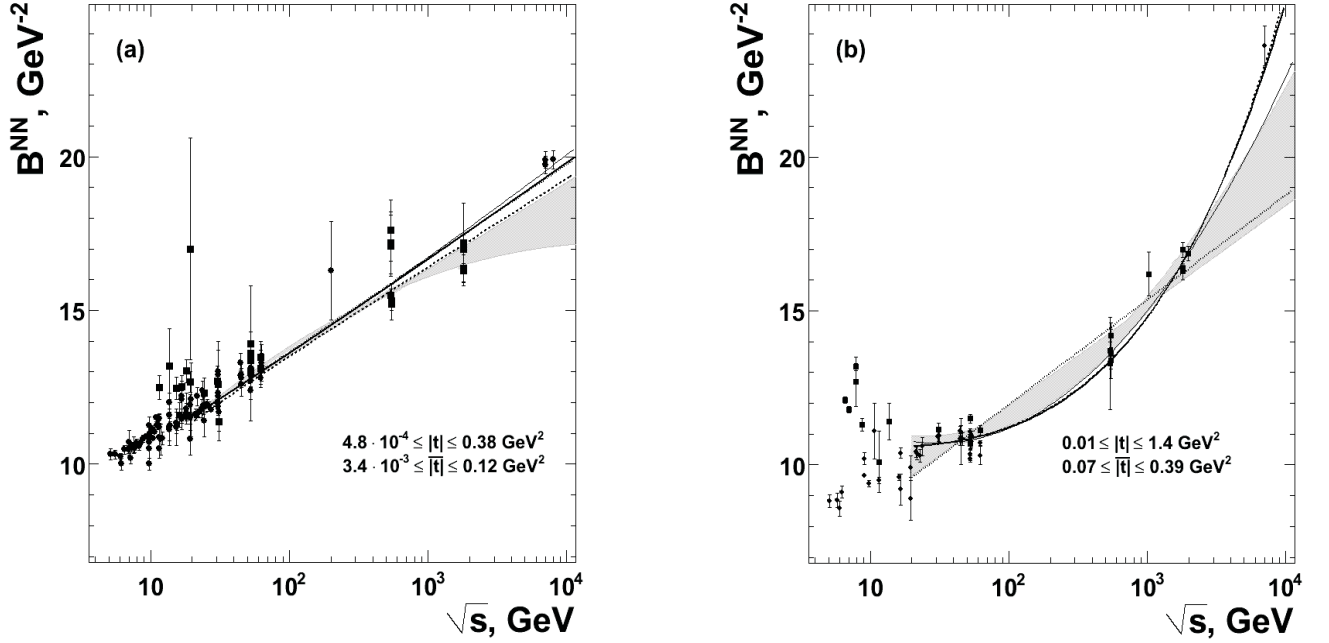


Fig. 4. Energy dependence of the elastic slope parameter in nucleon-nucleon scattering for low (a) and intermediate (b) domain of absolute values of momentum transfer. Experimental points from fitted samples are indicated as \bullet for pp and as \blacksquare for $\bar{p}p$. Fits are shown for $\sqrt{s_{\min}} = 20$ GeV. The dot curve is the fit of experimental slope by the function (2a), thick solid – by the (2b), dashed – by the (2c), thin solid – by the (2d). The shaded band corresponds to the spread of fitting functions for previous analysis [4].

above. We did not exclude any points from NN data sample, we change only the low energy boundary for fitted domain. Experimental data for slope in nucleon-nucleon elastic scattering against collision energy are shown in Fig.4a at low $|t|$ and in Fig.4b for intermediate $|t|$ together with fits by functions (2a) – (2d). We have fitted the general nucleon-nucleon data sample at range of low energy boundary $s_{\min} = 25, 100, 225$ and 400 GeV². The fit parameter values are indicated in Table 7 on the first line for low boundary of the fitted energy domain $s_{\min} = 25$ GeV² and on the second line – for $s_{\min} = 400$ GeV². The fit quality improves for most parameterizations under consideration at increasing of s_{\min} , thus fitting functions (2a) – (2d) are shown at Fig.4 for $s_{\min} = 400$ GeV². As seen from Fig.4a there is no experimental data for pp between $\sqrt{s} = 5$ GeV and $\sqrt{s} = 10$ GeV at low $|t|$. This energy domain will available for further FAIR facility. One need to emphasize the fit quality is some poorer ($\chi^2/\text{n.d.f.} \simeq 2.3 - 2.9$) at $\sqrt{s} \geq 10$ GeV than that for $\sqrt{s} \geq 5$ GeV for functions (2a) and (2c). For all cases of s_{\min} indicated above the value of the a_1 parameter obtained with the function (2a) agrees qualitatively with the prediction within the framework of Pomeron model, but the value of the asymptotic shrinkage parameter ($2\alpha'_{\mathcal{P}} = 0.662 \pm 0.010$) obtained at $s_{\min} = 400$ GeV² is some larger than the prediction for $\alpha'_{\mathcal{P}}$ from Pomeron inspired model for TeV-energy domain [94]. Also results from fit by function (2d) with acceptable quality at $s_{\min} = 400$ GeV² allow the estimation $2\alpha'_{\mathcal{P}}(s)|_{\sqrt{s}=8\text{TeV}} = 0.74 \pm 0.12$ which is some larger than the corresponding prediction from [94]. Furthermore the estimations for $2\alpha'_{\mathcal{P}}(s)|_{\sqrt{s}=8\text{TeV}}$ do not depend on s_{\min} within error bars. At low $|t|$ all functions (2a) – (2d) are close to each other at energies up to $\sqrt{s} \sim 1$ TeV at least and shows quasi-linear behavior for parameter values obtained by fits with $s_{\min} = 25$ GeV² and $s_{\min} = 400$ GeV². This observation confirms the suggestion that $B^{NN} \propto \ln \varepsilon$ at high \sqrt{s} at low $|t|$ values. As seen from comparison between the present fits and the spread of previous fit functions (shaded band) there is a dramatic change of behavior of the fitting function (2d) in comparison with previous analysis [4] due to experimental points at the LHC energies. At present the fitting function (2d) predicts increasing of the nuclear slope in high energy domain as well as all other fitting functions under study. Such behavior is opposite to the result of fit by function (2d) of experimental data sample at $\sqrt{s} \leq 1.8$ TeV [4]. We have analyzed the nucleon-nucleon data for slope parameter B at intermediate $|t|$ values for exponential parametrization with index linear in $|t|$ of $d\sigma/dt$ (Fig.4b). As seen experimental pp and $\bar{p}p$ data for B differ significantly up to $\sqrt{s} \simeq 10$ GeV at least that results in unacceptable fit qualities for all functions under study ($\chi^2/\text{n.d.f.} \simeq 28.9$ for best fit by quadratic in logarithm function). The Pomeron inspired function (2a) contradicts with experimental data at any s_{\min} . We would like to emphasize that the best fit quality for (2a) is obtained at $s_{\min} = 100$ GeV² ($\chi^2/\text{n.d.f.} \simeq 9.45$) but it is statistically unacceptable too. Functions (2b) – (2d) agree with experimental dependence $B(s)$ reasonably and have a close fit qualities. Furthermore the functions

(2b) and (2c) demonstrate very close behaviors in all range of \sqrt{s} under consideration. Best fit is "expanded" function (2c) in difference with previous analysis [4]. As seen from Fig.4b the slope parameter B increases much faster than $\ln \varepsilon$ at intermediate $|t|$ values. This result confirms the suggestion made on the base of the Fig.2 above and allows us to derive the asymptotic relation $B^{NN} \propto \ln^k \varepsilon, k > 2$ at high \sqrt{s} for intermediate $|t|$ domain. Fig.4b shows that the experimental point at the LHC energy leads to faster increasing of most of fitting functions in multi-TeV region in comparison with previous analysis [4]. Comparison between Fig.4a and Fig.4b demonstrates that the domain of intermediate $|t|$ is preferable with respect to the low $|t|$ range for discrimination of various phenomenological parameterizations for $B(s)$, in particular, the Pomeron inspired function (2a) from "expanded" ones. At $s_{\min} = 400$ GeV² and intermediate $|t|$ values the following estimations of asymptotic shrinkage parameter are obtained for fitting functions (2a) and (2d) respectively: $2\alpha'_{\mathcal{P}} = 0.706 \pm 0.012$ and $2\alpha'_{\mathcal{P}}(s)|_{\sqrt{s}=7\text{TeV}} = 1.9 \pm 0.2$. As well as for low $|t|$ domain the values of $\alpha'_{\mathcal{P}}$ are equal within errors at $\sqrt{s} = 7$ TeV and $\sqrt{s} = 8$ TeV in the case of the function (2d); the estimations for $2\alpha'_{\mathcal{P}}(s)|_{\sqrt{s}=7\text{TeV}}$ do not depend on s_{\min} within error bars. The growth of $\alpha'_{\mathcal{P}}$ is observed with increasing of $|t|$ ($|\bar{t}|$) values, especially, for fitting function (2d).

One can conclude the slope parameters for pp and $\bar{p}p$ elastic scattering show universal behavior at $\sqrt{s} \geq 20$ GeV and "expanded" functions represent the energy dependence for both the low and the intermediate $|t|$ ranges for this energy domain. Thus quantitative analysis of slopes at different $|t|$ allows us to get the following estimation of low energy boundary: $\sqrt{s} \simeq 20$ GeV for universality of elastic nucleon-nucleon scattering. This estimation agrees qualitatively with both the results for differential cross-sections of pp and $\bar{p}p$ elastic reactions based on the crossing-symmetry and derivative relations [1] and the results for global scattering parameters [104].

3 Conclusions

The present status of diffraction slope parameter for elastic pp and $\bar{p}p$ scattering is analyzed over the full energy domain as well as predictions for some facilities. The "expanded" parameterizations allow us to describe experimental B at all available energies in low $|t|$ domain for pp as well as for intermediate $|t|$ values for pp and $\bar{p}p$ quite reasonably. The similar situation is observed for fits of data samples joined for elastic NN scattering. Therefore "expanded" functions can be used as a reliable fits for wide range of momentum transfer at all energies. The new LHC data lead to dramatic change of behavior of quadratic in logarithm function and usually to better agreement between various fitting function in comparison with the analysis of pp data at $\sqrt{s} \leq 200$ GeV. At low values of $|t|$ the "standard" approximation differs from expanded ones and experimental data mostly in the low energy region; at intermediate $|t|$ this function is unacceptable for fitting of

Table 7. Values of parameters for fitting of slope energy dependence in NN elastic scattering

Function	Parameter				
	B_0, GeV^{-2}	a_1, GeV^{-2}	a_2, GeV^{-2}	a_3	$\chi^2/\text{n.d.f.}$
	low $ t $ domain				
(2a)	8.10 ± 0.05	0.301 ± 0.004	–	–	332/127
	7.55 ± 0.05	0.331 ± 0.005	–	–	103/63
(2b)	9.4 ± 0.2	6.1 ± 1.1	-12 ± 2	-3.5 ± 1.5	281/125
	8.1 ± 0.7	2.532 ± 0.006	-4.6 ± 0.2	0.988 ± 0.015	103/61
(2c)	8.15 ± 0.09	0.208 ± 0.010	0.50 ± 0.09	0.118 ± 0.005	281/125
	7.8 ± 0.2	0.323 ± 0.009	-7.0 ± 1.7	-0.65 ± 0.15	102/61
(2d)	8.81 ± 0.12	0.204 ± 0.015	0.011 ± 0.002	–	286/126
	8.0 ± 0.3	0.28 ± 0.04	0.005 ± 0.003	–	101/62
	intermediate $ t $ domain				
(2a)	8.25 ± 0.06	0.214 ± 0.004	–	–	3135/57
	5.17 ± 0.11	0.369 ± 0.006	–	–	353/36
(2b)	12.12 ± 0.10	-0.217 ± 0.11	0.0097 ± 0.0009	2.60 ± 0.04	1615/55
	10.7 ± 0.2	-0.019 ± 0.011	$(1.04 \pm 0.17) \times 10^{-4}$	4.08 ± 0.08	107/34
(2c)	4.43 ± 0.17	-0.602 ± 0.013	7.72 ± 0.16	0.0911 ± 0.0009	1613/55
	10.5 ± 0.2	-0.165 ± 0.019	0.66 ± 0.06	0.187 ± 0.004	106/34
(2d)	13.07 ± 0.14	-0.438 ± 0.017	0.0743 ± 0.0019	–	1617/56
	14.9 ± 0.6	-0.61 ± 0.06	0.089 ± 0.006	–	118/35

experimental NN data at all. The intermediate $|t|$ range is preferable with respect to the low $|t|$ values for discrimination of various phenomenological parameterizations for $B(s)$ dependence. Based on the nuclear slope the low energy boundary for universality of elastic nucleon-nucleon scattering is estimated as $\sqrt{s} \simeq 20$ GeV for both the low and the intermediate $|t|$ values that is in agreement with the hypothesis of a universal shrinkage of the hadronic diffraction cone at high energies. The difference of slopes for antiproton-proton and proton-proton elastic scattering (ΔB) shows the opposite behaviors at high energies for low and intermediate $|t|$ domains (decreasing / increasing, respectively) for all fitting functions with the exception of Pomeron inspired one. All underlying fitting functions with experimentally inspired values of parameters don't predict the zero value for ΔB at both the low and the intermediate $|t|$ ranges at high energies. Slop analysis of joined NN data samples allows us to estimate the asymptotic shrinkage parameter parameter for various domains of $|t|$. The estimation of the α'_P obtained with quadratic in logarithm function for NN data at $\sqrt{s} = 8$ TeV for low $|t|$ is noticeably larger than the expectation from the Pomeron theory. But the growth of α'_P with increasing of \sqrt{s} is observed from the comparison of the fit results from present study and our earlier analysis for $\sqrt{s} \leq 1.8$ TeV. The such behavior of α'_P agrees with Pomeron inspired model. The growth of α'_P is observed with increasing of momentum transfer. Based on the fit results the predictions for slope parameters B and b are obtained for elastic pp and $\bar{p}p$ scattering in energy domains of some facilities. It seems the phenomenological model with hadronic amplitude corresponding to the exchange of three pomerons describes the B some closer to the experimental fit inspired values at the LHC energy both at low and intermediate $|t|$ than other models.

Appendix

Experimental database for slope in nucleon-nucleon elastic scattering

In this Appendix, the numerical values used in the Sec. 2 are shown for diffractive slope parameter. The database includes the experimental values of the slope obtained with exponential approximations of $d\sigma/dt$ shown above. In the Tables 8 – 11 the statistical errors are shown by first and available systematic uncertainties are demonstrated by second. The compilation of some early experimental measurements of the slope in $pp/\bar{p}p$ elastic scattering at low energies was made in [5]. This one reference is shown and detail list of corresponding original papers can be found in [5]. In the case of $\bar{p}p$ elastic scattering in low $|t|$ domain (Table 10) the average \sqrt{s} are demonstrated for ranges of initial momentum (p_{lab}) 1.23 – 1.33 GeV/c and 1.45 – 1.65 GeV/c [5]. As for database of collective parameters [93] the results from latest paper of the experiment are included in Tables 8 – 11 below at certain \sqrt{s} and range of $|t|$. Measurements of particular experiment can be separated among Tables 8 – 11 in accordance with the limits for low / intermediate $|t|$ domain defined above. But here there is no averaging over results of various experiments at equal collision energy in difference with [93]. Furthermore the averaging over results in different ranges of $|t|$ for particular experiment at the same \sqrt{s} is absent too within the low / intermediate $|t|$ domain. Thus the measurements of particular experiment at fixed \sqrt{s} and in various ranges of $|t|$ are shown separately in the corresponding Table below if these measurements are in the chosen $|t|$ domain (see, for example, [22, 74, 78]) and agree with general trend, at least, qualitatively. Therefore the database includes the differential measurements over both the \sqrt{s} and the $|t|$ in the cases of some experiments.

References

1. S.B. Nurushev and V.A. Okorokov, Proceedings of the XII Advanced Research Workshop on High Energy Spin Physics. Dubna. 2008. P. 117. Eds. by A.V. Efremov and S.V. Goloskokov; arXiv: 0711.2231 [hep-ph]. 2007.
2. V.A. Okorokov, arXiv: 0811.0895 [hep-ph]. 2008.
3. V.A. Okorokov, arXiv: 0811.3849 [hep-ph]. 2008.
4. V.A. Okorokov, arXiv: 0907.0951 [hep-ph]. 2009.
5. T. Lasinski *et al.*, Nucl. Phys. **B37**, 1 (1972) and referencies therein.
6. D.W.G.S. Leihth, Preprint SLAC, N SLAC-PUB-1263 (T/E), 1973.
7. G. N. Velichko *et al.*, Pisma Zh. Eksp. Teor. Phys. **33**, 615 (1981).
8. V. V. Zhurkin *et al.*, Yad. Fiz. **28**, 1280 (1978).
9. G. G. Beznogikh *et al.*, Phys. Lett. **43B**, 85 (1973).
10. P. Jenni *et al.*, Nucl. Phys. **B129**, 232 (1977).
11. V. Bartenev *et al.*, Phys. Rev. Lett. **31**, 1088 (1973).
12. S. Bellettini *et al.*, Phys. Lett. **14**, 164 (1965).
13. R. K. Carnegie *et al.*, Phys. Lett. **59B**, 313 (1975).
14. G. G. Beznogikh *et al.*, Nucl. Phys. **B54**, 78 (1973).
15. V. Bartenev *et al.*, Phys. Rev. Lett. **29**, 1755 (1972).
16. I. M. Geshkov *et al.*, Phys. Rev. **D13**, 1846 (1976).
17. V. D. Apokin *et al.*, Yad. Fiz. **25**, 94 (1977).
18. D. S. Ayres *et al.*, Phys. Rev. **D15**, 3105 (1977).
19. L. A. Fajardo *et al.*, Phys. Rev. **D24**, 46 (1981).
20. R. L. Cool *et al.*, Phys. Rev. **D24**, 2821 (1981).
21. J. P. Burq *et al.*, Nucl. Phys. **B217**, 285 (1983).
22. S. Barish *et al.*, Phys. Rev. **D9**, 1171 (1974).
23. G. Barbiellini *et al.*, Phys. Lett. **39B**, 663 (1972).
24. J. P. Burq *et al.*, Phys. Lett. **109B**, 124 (1982).
25. N. Amos *et al.*, Nucl. Phys. **B262**, 689 (1985).
26. U. Amaldi *et al.*, Phys. Lett. **62B**, 460 (1976).
27. R. E. Breedon *et al.*, Phys. Lett. **B216**, 459 (1989).
28. M. Holder *et al.*, Phys. Lett. **36B**, 400 (1971).
29. L. Baksay *et al.*, Nucl. Phys. **B141**, 1 (1978).
30. D. Favart *et al.*, Phys. Rev. Lett. **47**, 1191 (1981).
31. U. Amaldi *et al.*, Phys. Lett. **36B**, 504 (1971).
32. A. Breakstone *et al.*, Nucl. Phys. **B248**, 253 (1984).
33. U. Amaldi *et al.*, Phys. Lett. **66B**, 390 (1977).
34. U. Amaldi *et al.*, Phys. Lett. **44B**, 112 (1973).
35. U. Amaldi, K. R. Schubert, Nucl. Phys. **B166**, 301 (1980).
36. M. Ambrosio *et al.*, Phys. Lett. **115B**, 495 (1982).
37. M. Ambrosio *et al.*, Phys. Lett. **113B**, 347 (1982).
38. S. Bultmann *et al.*, Phys. Lett. **B579**, 245 (2004).
39. G. Antchev *et al.*, Lett. J. Exp. Fron. Phys. **101**, 21002 (2013).
40. G. Aad *et al.*, Nucl. Phys. **B889**, 486 (2014).
41. G. Antchev *et al.*, Phys. Rev. Lett. **111**, 021001 (2013).
42. E. Colton *et al.* Phys. Rev. **D7**, 3267 (1973).
43. D. Harting *et al.*, Nuovo Cim. **38**, 60 (1965).
44. R. M. Edelstein *et al.* Phys. Rev. **D5**, 1073 (1972).
45. S.B. Nurushev *et al.* (SIGMA Collaboration), Proceedings of the XVII International Conference on High Energy Physics. Rutherford Lab. V. **I**, 1974. P. I-25.
46. A. N. Diddens, Proceedings of the XVII International Conference on High Energy Physics. Rutherford Lab. V. **I**, 1974. P. I-41.
47. C. Bromberg *et al.* Phys. Rev. **D15**, 64 (1977).
48. D. Brick *et al.* Phys. Rev. **D25**, 2794 (1982).
49. N. Kwak *et al.* Phys. Lett. **58B**, 233 (1975).
50. A. Firestone *et al.* Phys. Rev. **D10**, 2080 (1974).
51. M. Holder *et al.* (ACGHT Collaboration) Phys. Lett. **35B**, 355 (1971).
52. H. De Kerret *et al.* Phys. Lett. **68B**, 374 (1977).
53. G. Antchev *et al.* (TOTEM Collaboration), Lett. J. Exp. Fron. Phys. **95**, 41001 (2011).
54. I. Ambats *et al.* Phys. Rev. **D10**, 2080 (1974).
55. K. J. Foley *et al.* Phys. Rev. Lett. **11**, 425 (1963).
56. K. J. Foley *et al.* Phys. Rev. Lett. **15**, 45 (1965).
57. C. Bromberg *et al.*, Phys. Rev. Lett. **31**, 1563 (1973).
58. W. Brückner *et al.*, Phys. Lett. **158B**, 180 (1985).
59. L. Linsen *et al.*, Nucl. Phys. **A469**, 726 (1987).
60. H. Iwasaki *et al.*, Nucl. Phys. **A433**, 580 (1985).
61. M. Cresti *et al.*, Phys. Lett. **132B**, 209 (1983).
62. V. Ashford *et al.*, Phys. Rev. Lett. **54**, 518 (1985).
63. P. Schiavon *et al.*, Nucl. Phys. **A505**, 595 (1989).
64. H. Kaseno *et al.*, Phys. Lett. **61B**, 203 (1976).
65. P. Jenni *et al.*, Nucl. Phys. **B94**, 1 (1975).
66. T. A. Armstrong *et al.* (E760 Collaboration), Phys. Lett. **B385**, 479 (1996).
67. P. S. Gregory *et al.*, Nucl. Phys. **B119**, 60 (1977).
68. N. Amos *et al.*, Phys. Lett. **128B**, 343 (1983).
69. N. Amos *et al.*, Phys. Lett. **120B**, 460 (1983).
70. R. Battiston *et al.* (UA4 Collaboration), Phys. Lett. **115B**, 333 (1982).
71. R. Battiston *et al.* (UA4 Collaboration), Phys. Lett. **127B**, 472 (1983).
72. G. Arnison *et al.* (UA1 Collaboration), Phys. Lett. **128B**, 336 (1983).
73. C. Augier *et al.* (UA4/2 Collaboration), Phys. Lett. **B316**, 448 (1993).
74. M. Bozzo *et al.* (UA4 Collaboration), Phys. Lett. **147B**, 385 (1984).
75. F. Abe *et al.* (CDF Collaboration), Phys. Rev. **D50**, 5518 (1994).
76. N. A. Amos *et al.* (E710 Collaboration), Phys. Rev. Lett. **61**, 525 (1988).
77. N. A. Amos *et al.* (E710 Collaboration), Phys. Rev. Lett. **63**, 2784 (1989).
78. N. A. Amos *et al.* (E710 Collaboration), Phys. Lett. **B247**, 127 (1990).
79. N. A. Amos *et al.* (E710 Collaboration), Phys. Rev. Lett. **68**, 2433 (1992).
80. H. Braun *et al.*, Nucl. Phys. **B95**, 481 (1975).
81. K. J. Foley *et al.* Phys. Rev. Lett. **11**, 503 (1963).
82. D. Birnbaum *et al.* Phys. Rev. Lett. **23**, 663 (1969).
83. B. V. Batyunya *et al.*, Yad. Phys. **44**, 1489 (1986).
84. Yu.,M. Antipov *et al.*, Nucl. Phys. **B57**, 333 (1973).
85. M. Yu. Bogolyubsky *et al.*, Yad. Phys. **41**, 1210 (1984).
86. F. Grard *et al.* Phys. Lett. **59B**, 409 (1975).
87. J. J. Dumont *et al.* Z. Phys. **C13**, 1 (1982).
88. R. E. Ansorge *et al.* Phys. Lett. **59B**, 299 (1975).
89. G. Arnison *et al.* (UA1 Collaboration), Phys. Lett. **121B**, 77 (1983).
90. N. A. Amos *et al.* (E710 Collaboration), Nuovo Cim. **A106**, 123 (1993).
91. V. M. Abazov *et al.* (D0 Collaboration), Phys. Rev. **D86**, 012009 (2012).
92. I. Ambast *et al.*, Phys. Rev. **D9**, 1179 (1974).
93. V.A. Okorokov, Int. J. Mod. Phys. **A27**, 1250037 (2012).
94. V.A. Schegelsky, M.G. Ryskin, Phys. Rev. **D85**, 094024 (2012).
95. G. Giacomelli, Phys. Rep. **23**, 123 (1976).

96. A.N. Skrinsky, Proceedings of the XXXIII International Conference on High Energy Physics. World Scientific. V. **I**, 2007. P. 175. Eds. by A. Sissakian, G. Kozlov and E. Koganova.
97. M.M. Block and R.N. Cahn, Rev. Mod. Phys. **57**, 563 (1985).
98. V. Kundrať, J. Kašpar and M. Lokajíček, Proceedings of the XII International Conference on Elastic and Diffractive Scattering Forward Physics and QCD. Verlag DESY. 2007. P. 273. Eds. by J. Bartels, M. Diehl and H. Jung.
99. M.M. Block, E.M. Gregores, F. Halzen and G. Pancheri, Phys. Rev. **D60**, 054024 (1999).
100. V.A. Petrov, E. Predazzi and A.V. Prokhudin, Eur. Phys. J. **C28**, 525 (2003).
101. C. Bourrely, J. Soffer and T.T. Wu, Eur. Phys. J. **C28**, 97 (2003).
102. M.M. Islam, R.J. Luddy and A.V. Prokhudin, Phys. Lett. **B605**, 115 (2005).
103. O.V. Selyugin and J.-R. Cudell, Proceedings of the XII International Conference on Elastic and Diffractive Scattering Forward Physics and QCD. Verlag DESY. 2007. P. 279. Eds. by J. Bartels, M. Diehl and H. Jung.
104. S.D. Campos and V.A. Okorokov, Int. J. Mod. Phys. **A25**, 5333 (2010).

Table 8. Experimental B_{pp} for low $|t|$ domain

\sqrt{s} , GeV	B_{pp} , GeV $^{-2}$	Ref.	\sqrt{s} , GeV	B_{pp} , GeV $^{-2}$	Ref.	\sqrt{s} , GeV	B_{pp} , GeV $^{-2}$	Ref.
1.962	1.60 ± 0.60	[5]	6.977	10.70 ± 0.40	[15]	19.42	10.80 ± 0.50	[15]
1.974	1.43 ± 0.41	[6]	7.167	10.20 ± 0.20	[12]	19.42	11.50 ± 0.40	[20]
1.993	0.40 ± 0.50	[5]	7.311	$10.52 \pm 0.12 \pm 0.30$	[14]	19.46	$11.93 \pm 0.05 \pm 0.32$	[19]
2.000	0.38 ± 0.19	[6]	7.620	10.61 ± 0.27	[16]	19.66	12.10 ± 1.20	[22]
2.002	0.60 ± 0.20	[5]	7.664	$10.49 \pm 0.12 \pm 0.30$	[14]	21.22	$11.61 \pm 0.19 \pm 0.20$	[11]
2.069	0.99 ± 0.38	[6]	8.019	$10.69 \pm 0.12 \pm 0.30$		21.49	11.57 ± 0.03	[23]
2.069	1.46 ± 0.47		8.345	$10.57 \pm 0.11 \pm 0.30$		21.70	12.20 ± 0.30	[24]
2.083	0.64 ± 0.29		8.550	$10.68 \pm 0.09 \pm 0.30$		22.55	$11.69 \pm 0.10 \pm 0.20$	[11]
2.125	2.63 ± 0.37		8.832	$10.82 \pm 0.11 \pm 0.30$		23.50	11.80 ± 0.30	[25]
2.177	3.56 ± 1.09	[7]	9.030*	13.50 ± 0.74	[17]	23.60	11.80 ± 0.30	[26]
2.218	4.42 ± 0.51		9.303	$10.90 \pm 0.09 \pm 0.30$	[14]	23.76	12.40 ± 0.30	[24]
2.239	5.83 ± 0.39		9.777	10.50 ± 0.40	[15]	24.23	$11.90 \pm 0.28 \pm 0.20$	[11]
2.259	4.88 ± 0.45		9.777	11.25 ± 0.28	[16]	24.30	$11.40 \pm 0.50 \pm 0.07$	[27]
2.279	5.53 ± 0.46		9.778	$10.70 \pm 0.18 \pm 0.20$	[11]	25.59	$11.96 \pm 0.15 \pm 0.20$	[11]
2.300	6.49 ± 0.60		9.778	$10.00 \pm 0.20 \pm 0.15$	[18]	26.42	$11.87 \pm 0.15 \pm 0.20$	
2.319	6.24 ± 0.37		9.837	$10.84 \pm 0.11 \pm 0.30$	[14]	27.29	$11.77 \pm 0.10 \pm 0.20$	
2.465	5.70 ± 0.60	[5]	9.977	$11.00 \pm 0.12 \pm 0.30$		30.48	12.00 ± 0.20	[28]
2.465	5.97 ± 0.15	[8]	9.987*	12.70 ± 0.70	[17]	30.60	12.00 ± 0.20	[29]
2.696	7.80 ± 0.50	[5]	10.19	$11.12 \pm 0.13 \pm 0.30$	[14]	30.60	12.20 ± 0.30	[25]
2.702	7.60 ± 0.43	[9]	10.43	$11.11 \pm 0.10 \pm 0.30$		30.70	12.90 ± 1.10	[30]
2.725	7.80 ± 0.37	[6]	10.52	$10.83 \pm 0.07 \pm 0.20$	[11]	30.80	12.30 ± 0.30	[26]
2.735	6.50 ± 0.60	[5]	10.71	$11.05 \pm 0.08 \pm 0.30$	[14]	30.81	11.87 ± 0.28	[23]
2.987	8.33 ± 0.37		11.00	$11.50 \pm 0.11 \pm 0.30$	[9]	30.82	13.00 ± 0.70	[31]
3.266	7.69 ± 0.37	[6]	11.17	$11.50 \pm 0.11 \pm 0.30$	[14]	31.00	11.70 ± 0.62	[32]
3.307	7.80 ± 0.44	[9]	11.22	$11.24 \pm 0.11 \pm 0.30$		44.70	12.80 ± 0.30	[33]
3.321	7.70 ± 0.50	[5]	11.47	$11.46 \pm 0.09 \pm 0.30$		44.87	12.87 ± 0.20	[23]
3.843	9.60 ± 0.30		11.53	$11.48 \pm 0.15 \pm 0.30$		44.90	13.30 ± 0.30	[29]
3.851	9.14 ± 0.35	[9]	11.54	11.21 ± 0.40	[16]	45.00	12.60 ± 0.40	[34]
3.874*	8.20 ± 0.20	[5]	11.54	$10.50 \pm 0.30 \pm 0.16$	[18]	45.00	12.80 ± 0.30	[26]
3.875	9.40 ± 0.60	[10]	11.54	$10.87 \pm 0.14 \pm 0.34$	[19]	45.06	12.90 ± 0.40	[31]
3.995	9.53 ± 0.23	[6]	11.94	10.80 ± 0.50	[15]	52.80	13.10 ± 0.20	[29]
4.305	9.52 ± 0.26	[5]	12.17	$10.84 \pm 0.20 \pm 0.20$	[11]	52.80	13.10 ± 0.20	[35]
4.307	9.40 ± 0.30	[9]	13.76	11.60 ± 0.50	[15]	52.80	12.70 ± 0.20	[30]
4.329	$8.72 \pm 0.38 \pm 0.20$	[11]	13.76	11.20 ± 0.60	[20]	52.80	$13.09 \pm 0.37 \pm 0.21$	[36]
4.478	9.50 ± 0.22	[6]	13.76	$11.13 \pm 0.14 \pm 0.33$	[19]	52.80	12.87 ± 0.14	[25]
4.540	9.20 ± 0.40	[10]	13.76	12.00 ± 0.30	[21]	52.90	13.10 ± 0.30	[33]
4.562	10.40 ± 0.40	[12]	13.90	$11.24 \pm 0.13 \pm 0.20$	[11]	52.99	12.40 ± 0.30	[23]
4.621	$8.90 \pm 0.17 \pm 0.10$	[13]	15.36	$11.34 \pm 0.09 \pm 0.33$	[19]	53.00	13.10 ± 0.30	[34]
4.721	9.25 ± 0.45	[5]	15.37	11.20 ± 0.60	[15]	53.10	13.00 ± 0.30	[31]
4.721	9.16 ± 0.37	[9]	15.56	$11.30 \pm 0.20 \pm 0.20$	[11]	62.30	13.02 ± 0.27	[25]
4.934	$9.03 \pm 0.30 \pm 0.20$	[11]	16.26	$11.60 \pm 0.40 \pm 0.17$	[18]	62.40	13.30 ± 0.30	[33]
4.953	10.80 ± 1.00	[5]	16.83	12.20 ± 0.50	[15]	62.50	12.80 ± 0.20	[29]
4.953	9.24 ± 0.35	[6]	16.83	$11.57 \pm 0.23 \pm 0.20$	[11]	63.00	13.30 ± 0.60	[37]
5.150	$10.32 \pm 0.17 \pm 0.30$	[14]	16.83	12.10 ± 0.30	[21]	200.0	$16.30 \pm 1.60 \pm 0.90$	[38]
5.562	$10.31 \pm 0.15 \pm 0.30$		16.91	$11.46 \pm 0.06 \pm 0.33$	[19]	7000	$19.89 \pm 0.02 \pm 0.27$	[39]
6.105	$10.24 \pm 0.11 \pm 0.30$		18.14	$11.63 \pm 0.09 \pm 0.33$		7000	$19.73 \pm 0.14 \pm 0.26$	[40]
6.171	10.00 ± 0.20	[12]	18.17	11.80 ± 0.50	[15]	8000	19.90 ± 0.30	[41]
6.522	$10.47 \pm 0.14 \pm 0.30$	[14]	18.17	$11.52 \pm 0.11 \pm 0.20$	[11]			
6.920	$10.48 \pm 0.13 \pm 0.30$		19.37	$11.56 \pm 0.12 \pm 0.20$				

*The point is excluded from the fit procedure.

Table 9. Experimental B_{pp} for intermediate $|t|$ domain

\sqrt{s} , GeV	B_{pp} , GeV $^{-2}$	Ref.	\sqrt{s} , GeV	B_{pp} , GeV $^{-2}$	Ref.	\sqrt{s} , GeV	B_{pp} , GeV $^{-2}$	Ref.
Linear parameterization $\ln(d\sigma/dt) \propto (-B t)$								
2.034	1.60 ± 0.60	[5]	3.942	7.37 ± 0.29		23.00	10.30 ± 0.20	[49]
2.037	0.20 ± 1.40		4.220	7.75 ± 0.11	[43]	23.76	10.60 ± 0.30	[50]
2.058	0.59 ± 0.11		4.331	8.39 ± 20	[6]	30.81	10.91 ± 0.22	[23]
2.066	1.00 ± 0.50		4.519	8.95 ± 0.06	[44]	31.00	10.92 ± 0.15	[32]
2.075	0.00 ± 0.70		4.621	$8.11 \pm 0.17 \pm 0.10$	[13]	31.39	10.93 ± 0.20	[6]
2.098	0.90 ± 0.40		4.694	8.53 ± 0.22	[6]	44.61	11.10 ± 0.15	[28]
2.112	0.40 ± 0.60		5.010*	8.19 ± 0.13	[43]	44.87	10.83 ± 0.20	[23]
2.132	1.50 ± 0.60		5.122	8.83 ± 20	[6]	45.00	10.75 ± 0.75	[51]
2.142	1.20 ± 0.40		5.780	8.86 ± 23		45.41	11.08 ± 0.20	[6]
2.153	1.30 ± 0.30		6.028	8.58 ± 0.24	[43]	46.34	10.84 ± 0.20	
2.166	3.00 ± 0.50		6.223	9.12 ± 0.19	[6]	52.61	10.90 ± 0.15	[28]
2.180	2.70 ± 0.50		9.081	9.65 ± 0.07	[45]	52.80	10.70 ± 0.20	[35]
2.191	3.60 ± 0.60		9.081	10.20 ± 20	[46]	52.80	$10.34 \pm 0.19 \pm 0.06$	[36]
2.201*	5.10 ± 0.60		9.778	$9.40 \pm 0.10 \pm 0.14$	[18]	52.99	10.80 ± 0.20	[23]
2.688	5.55 ± 0.20	[6]	10.69	11.10 ± 0.90	[47]	53.00	11.06 ± 0.11	[32]
2.780	6.46 ± 0.25		11.54	$9.50 \pm 0.10 \pm 0.14$	[18]	53.00	10.20 ± 0.10	[52]
2.837	5.55 ± 0.23		16.26	$9.60 \pm 0.10 \pm 0.14$		53.35	10.78 ± 0.23	[6]
3.034	6.25 ± 0.26		16.66	10.38 ± 0.17		54.44	10.93 ± 0.18	
3.363	7.12 ± 0.11	[5]	16.66	9.20 ± 0.50	[48]	62.00	10.30 ± 0.30	[49]
3.378	7.37 ± 0.25	[6]	19.66	8.90 ± 0.70	[22]	62.00	10.71 ± 0.08	[32]
3.433	7.60 ± 0.50	[5]	19.66	9.90 ± 0.40		7000	$23.60 \pm 0.50 \pm 0.40$	[53]
3.778	7.94 ± 0.26	[42]	21.49	10.42 ± 0.17	[23]			
3.916	7.95 ± 0.18	[6]	21.84	10.38 ± 0.22	[6]			
Quadratic parameterization $\ln(d\sigma/dt) \propto (-B t \pm Ct^2)$								
2.212	4.60 ± 0.90	[5]	3.826	9.78 ± 0.21	[55]	6.272	9.17 ± 0.11	[44]
2.236	5.50 ± 0.70		4.131	7.00 ± 1.10	[5]	6.434	9.50 ± 0.90	[5]
2.265	6.40 ± 0.60		4.220	8.16 ± 0.28	[43]	6.434	9.80 ± 0.30	
2.272	7.64 ± 0.46		4.220	8.35 ± 0.25		6.477	10.90 ± 0.60	
2.304	6.50 ± 0.60		4.286	9.62 ± 0.22	[55]	6.547	9.63 ± 0.78	[56]
2.307	8.12 ± 0.84		4.701	9.79 ± 0.23		6.871	9.90 ± 1.00	[5]
2.311	6.50 ± 0.80		4.729	8.56 ± 0.47	[56]	6.929	7.97 ± 1.56	[56]
2.325	7.70 ± 0.30		5.010	9.05 ± 0.34	[43]	7.138	11.60 ± 0.70	[5]
2.339	6.30 ± 0.50		5.010	9.71 ± 0.16		7.422	9.10 ± 1.10	
2.342	8.80 ± 1.00		5.084	10.03 ± 0.28	[55]	7.584	9.34 ± 0.28	[44]
2.360	5.70 ± 0.50		5.120	9.90 ± 1.10	[5]	9.081*	11.20 ± 0.22	[45]
2.395	6.30 ± 0.40		5.128	11.40 ± 1.20		9.778	$10.30 \pm 0.10 \pm 0.15$	[18]
2.458	7.10 ± 0.40		5.440	10.37 ± 0.33	[55]	11.54	$10.60 \pm 0.20 \pm 0.16$	
2.510	7.30 ± 1.00		5.462	8.89 ± 0.52	[56]	13.76	$10.70 \pm 0.20 \pm 0.16$	
2.682	8.10 ± 0.40		5.491	8.81 ± 0.25	[44]	13.90	11.40 ± 0.70	[57]
2.768	6.10 ± 0.90		5.559	10.00 ± 0.80	[5]	16.26	$11.30 \pm 0.10 \pm 0.17$	[18]
2.768	7.20 ± 0.20		5.757	9.79 ± 0.40	[55]	18.17	$11.30 \pm 0.10 \pm 0.17$	
2.768	7.80 ± 0.15	[54]	5.981	9.60 ± 0.90	[5]	19.46*	12.64 ± 0.12	[19]
2.972	8.29 ± 0.16		6.028	9.79 ± 0.63	[43]	27.60	10.70 ± 0.90	[57]
2.978	6.60 ± 0.70	[5]	6.028	9.96 ± 0.21		31.00*	12.83 ± 0.34	[32]
3.077	8.20 ± 1.00		6.059*	12.50 ± 0.70	[5]	53.00	10.09 ± 0.47	
3.363	8.46 ± 0.16	[54]	6.123	9.06 ± 0.22		62.00	10.12 ± 2.90	
3.497	8.70 ± 0.50	[5]	6.212	10.48 ± 0.43	[55]			
3.627	8.46 ± 0.16	[54]	6.248	8.68 ± 0.79	[56]			

*The point is excluded from the fit procedure.

Table 10. Experimental $B_{\bar{p}p}$ for low $|t|$ domain

\sqrt{s} , GeV	$B_{\bar{p}p}$, GeV $^{-2}$	Ref.	\sqrt{s} , GeV	$B_{\bar{p}p}$, GeV $^{-2}$	Ref.	\sqrt{s} , GeV	$B_{\bar{p}p}$, GeV $^{-2}$	Ref.
1.885	83.70 ± 24.00	[58]	1.946	26.60 ± 3.20	[5]	2.638	13.10 ± 0.40	[65]
1.887	129.0 ± 25.00	[5]	1.946	23.30 ± 1.10	[61]	2.669	13.10 ± 0.30	[5]
1.889	61.20 ± 16.50	[58]	1.948	22.00 ± 2.00	[60]	2.957	14.10 ± 1.60	
1.891	62.30 ± 7.40	[5]	1.949	19.12 ± 0.83	[62]	2.987	$12.90 \pm 0.39 \pm 0.08$	[66]
1.891	52.40 ± 3.80	[58]	1.950	20.90 ± 2.10	[63]	3.077	13.50 ± 0.90	[5]
1.891	$71.50 \pm 4.50 \pm 7.00$	[59]	1.951	25.90 ± 1.70	[5]	3.098	$12.80 \pm 0.70 \pm 0.08$	[66]
1.892	38.80 ± 1.30	[60]	1.951	21.00 ± 1.10	[61]	3.524	$12.50 \pm 0.29 \pm 0.08$	
1.894	39.20 ± 2.00	[58]	1.951	24.70 ± 0.60	[60]	3.555	$12.20 \pm 0.39 \pm 0.08$	
1.896	51.20 ± 4.60	[5]	1.956	24.80 ± 1.20	[5]	3.612	$12.60 \pm 0.29 \pm 0.08$	
1.896	40.50 ± 0.90	[60]	1.957	22.20 ± 1.10	[61]	3.627	13.50 ± 0.90	[10]
1.896	$47.70 \pm 2.70 \pm 5.00$	[59]	1.957	24.10 ± 0.60	[60]	3.686	$12.20 \pm 0.59 \pm 0.08$	[66]
1.898	32.30 ± 1.70	[58]	1.960	23.40 ± 0.60		4.108	12.66 ± 0.05	[5]
1.900	39.00 ± 2.00	[60]	1.960	22.80 ± 0.94	[58]	4.108	13.00 ± 0.50	[10]
1.901	45.10 ± 4.10	[5]	1.962	24.90 ± 1.20	[5]	4.351	13.00 ± 0.10	[67]
1.902	35.70 ± 0.80	[60]	1.962	18.79 ± 0.80	[62]	4.540	11.80 ± 3.00	[5]
1.906	42.20 ± 4.80	[5]	1.969	18.23 ± 0.80		4.540	12.20 ± 0.10	[10]
1.907	36.50 ± 0.80	[60]	1.973	20.40 ± 2.20	[5]	4.621	$11.38 \pm 0.17 \pm 0.10$	[13]
1.908	32.10 ± 3.50	[5]	1.976	21.73 ± 0.85	[62]	11.54	$12.49 \pm 0.18 \pm 0.33$	[19]
1.908	33.50 ± 1.20	[61]	1.985	15.90 ± 0.80	[60]	13.76	13.20 ± 1.20	[20]
1.909	44.15 ± 5.55	[62]	1.989	15.00 ± 1.80	[64]	15.36	$12.46 \pm 0.14 \pm 0.33$	[19]
1.911	28.60 ± 6.80	[5]	1.994	12.00 ± 2.00	[60]	16.91	$12.52 \pm 0.16 \pm 0.33$	
1.912	33.60 ± 1.70	[60]	1.996	14.10 ± 2.60	[5]	18.14	$13.03 \pm 0.19 \pm 0.33$	
1.917	27.40 ± 1.70	[62]	2.005	16.30 ± 1.20		19.42	17.00 ± 3.60	[20]
1.918	24.80 ± 2.60	[5]	2.006	18.00 ± 0.50	[63]	19.46	$12.68 \pm 0.10 \pm 0.32$	[19]
1.918	28.80 ± 1.20	[61]	2.036	18.60 ± 1.50	[5]	24.30	$12.30 \pm 0.50 \pm 0.07$	[27]
1.920	29.10 ± 0.50	[60]	2.107	15.20 ± 0.30	[63]	30.40	12.70 ± 0.50	[25]
1.921	22.70 ± 4.20	[5]	2.115	16.10 ± 0.40	[60]	30.70	12.60 ± 0.30	[68]
1.922	24.70 ± 1.70	[60]	2.138	15.00 ± 0.30		31.00	11.37 ± 0.60	[32]
1.923	22.63 ± 1.30	[62]	2.140	14.90 ± 0.60	[65]	52.60	13.03 ± 0.52	[25]
1.926	23.80 ± 2.30	[5]	2.159	14.20 ± 0.30	[60]	52.80	13.60 ± 2.20	[30]
1.926	26.80 ± 1.20	[61]	2.184	15.20 ± 0.30		52.80	$13.92 \pm 0.37 \pm 0.22$	[36]
1.926	26.20 ± 0.50	[60]	2.193	15.40 ± 0.30		52.80	13.36 ± 0.53	[69]
1.927	23.38 ± 1.15	[62]	2.204	14.50 ± 0.30		62.30	13.47 ± 0.52	[25]
1.931	22.30 ± 1.50	[5]	2.221	14.20 ± 0.20		62.50	13.10 ± 0.60	[68]
1.931	23.70 ± 0.40	[60]	2.223	14.20 ± 0.30	[65]	540.0	17.20 ± 1.00	[70]
1.932	22.52 ± 1.05	[62]	2.227	15.80 ± 0.30	[60]	540.0	17.60 ± 1.00	[71]
1.933	23.80 ± 1.20	[61]	2.254*	5.20 ± 0.30		540.0	17.10 ± 1.00	[72]
1.936	21.80 ± 0.60	[60]	2.260	16.50 ± 0.40		541.0	15.50 ± 0.20	[73]
1.938	18.80 ± 1.90	[5]	2.292	15.10 ± 1.80	[5]	546.0	15.30 ± 0.30	[74]
1.938	18.98 ± 0.90	[62]	2.294	12.40 ± 0.50	[60]	546.0	15.20 ± 0.20	
1.939	26.40 ± 1.14	[58]	2.296	14.40 ± 0.40	[5]	546.0	$15.28 \pm 0.28 \pm 0.09$	[75]
1.940	25.20 ± 1.10	[61]	2.304*	5.90 ± 0.30	[60]	1800	17.20 ± 1.30	[76]
1.942	22.40 ± 2.70	[5]	2.325	13.30 ± 1.30	[5]	1800	16.30 ± 0.50	[77]
1.943	20.01 ± 0.82	[62]	2.348	13.30 ± 0.20	[60]	1800	16.37 ± 0.45	[78]
1.944	20.10 ± 2.20	[5]	2.352	13.20 ± 0.30	[65]	1800	16.99 ± 0.47	[79]
1.945	22.80 ± 0.40	[60]	2.430	15.60 ± 1.40	[5]			

*The point is excluded from the fit procedure.

Table 11. Experimental $B_{\bar{p}p}$ for intermediate $|t|$ domain

\sqrt{s} , GeV	$B_{\bar{p}p}$, GeV ⁻²	Ref.	\sqrt{s} , GeV	$B_{\bar{p}p}$, GeV ⁻²	Ref.	\sqrt{s} , GeV	$B_{\bar{p}p}$, GeV ⁻²	Ref.
Linear parameterization $\ln(d\sigma/dt) \propto (-B t)$								
2.156*	17.80 ± 0.40	[5]	4.307	12.83 ± 0.21	[5]	31.00	11.16 ± 0.20	[32]
2.177	11.80 ± 1.00		4.540	11.80 ± 2.90	[81]	52.80	10.68 ± 0.20	[36]
2.271	11.20 ± 1.30		4.621	12.09 ± 0.24 ± 0.10	[13]	53.00	11.50 ± 0.15	[32]
2.335	16.50 ± 1.00		4.896	12.33 ± 0.79	[56]	62.00	11.12 ± 0.15	
2.465	12.90 ± 0.70		4.896	12.30 ± 0.80	[5]	540.0	13.30 ± 1.50	[89]
2.558	13.40 ± 1.10		4.934	12.66 ± 0.29	[81]	540.0	13.70 ± 0.30	[71]
2.702	13.00 ± 2.30		4.934	12.70 ± 0.30	[5]	540.0	13.70 ± 0.20 ± 0.20	[72]
2.768	13.00 ± 0.80		5.627*	8.78 ± 1.00	[56]	546.0	13.40 ± 0.30	[74]
2.857	13.10 ± 0.70		5.642*	11.44 ± 0.20	[82]	546.0	13.60 ± 0.80	
3.550	12.10 ± 0.40		5.642*	11.64 ± 0.08	[5]	546.0	14.20 ± 0.40	
3.550	12.60 ± 0.20	[80]	6.621	13.10 ± 0.80	[83]	546.0*	15.35 ± 0.18 ± 0.06	[75]
3.851*	15.60 ± 0.40	[5]	7.006	11.80 ± 0.10 ± 0.12	[84]	1020	16.20 ± 0.50 ± 0.50	[90]
3.923	13.15 ± 0.47	[81]	7.864	13.26 ± 0.30	[85]	1800	16.30 ± 0.30	[78]
3.923	13.10 ± 0.40	[5]	7.875	12.70 ± 0.80	[86]	1800	16.40 ± 0.12	
4.108	12.57 ± 0.20	[82]	8.777	11.30 ± 0.20 ± 0.11	[84]	1800	16.98 ± 0.24 ± 0.07	[75]
4.108	12.72 ± 0.11	[5]	11.54	10.10 ± 1.00	[87]	1960	16.86 ± 0.10 ± 0.20	[91]
4.307	12.84 ± 0.21	[81]	13.76	11.40 ± 0.60	[88]			
Quadratic parameterization $\ln(d\sigma/dt) \propto (-B t \pm Ct^2)$								
2.768	12.20 ± 0.80	[92]	8.777	12.20 ± 0.70 ± 0.12	[84]	31.00	13.06 ± 0.39	[32]
2.972	12.10 ± 1.00		9.778	12.60 ± 0.20 ± 0.19	[18]	53.00*	10.96 ± 0.44	
3.363	11.40 ± 1.00		11.54	12.80 ± 0.30 ± 0.19		62.00*	11.30 ± 0.45	
3.627	12.40 ± 1.50		13.76	11.90 ± 0.50 ± 0.18		1800	16.25 ± 0.23	[78]
6.621	13.10 ± 0.80	[83]	16.26	12.60 ± 0.40 ± 0.19		1800	16.87 ± 0.57	
7.006	12.80 ± 0.40 ± 0.13	[84]	18.17	13.10 ± 0.40 ± 0.20		1800	20.65 ± 3.84	
7.864	13.26 ± 0.30	[85]	19.46*	13.27 ± 0.24	[19]			

*The point is excluded from the fit procedure.